:Lecture 27: Stellar Nucleosynthesis

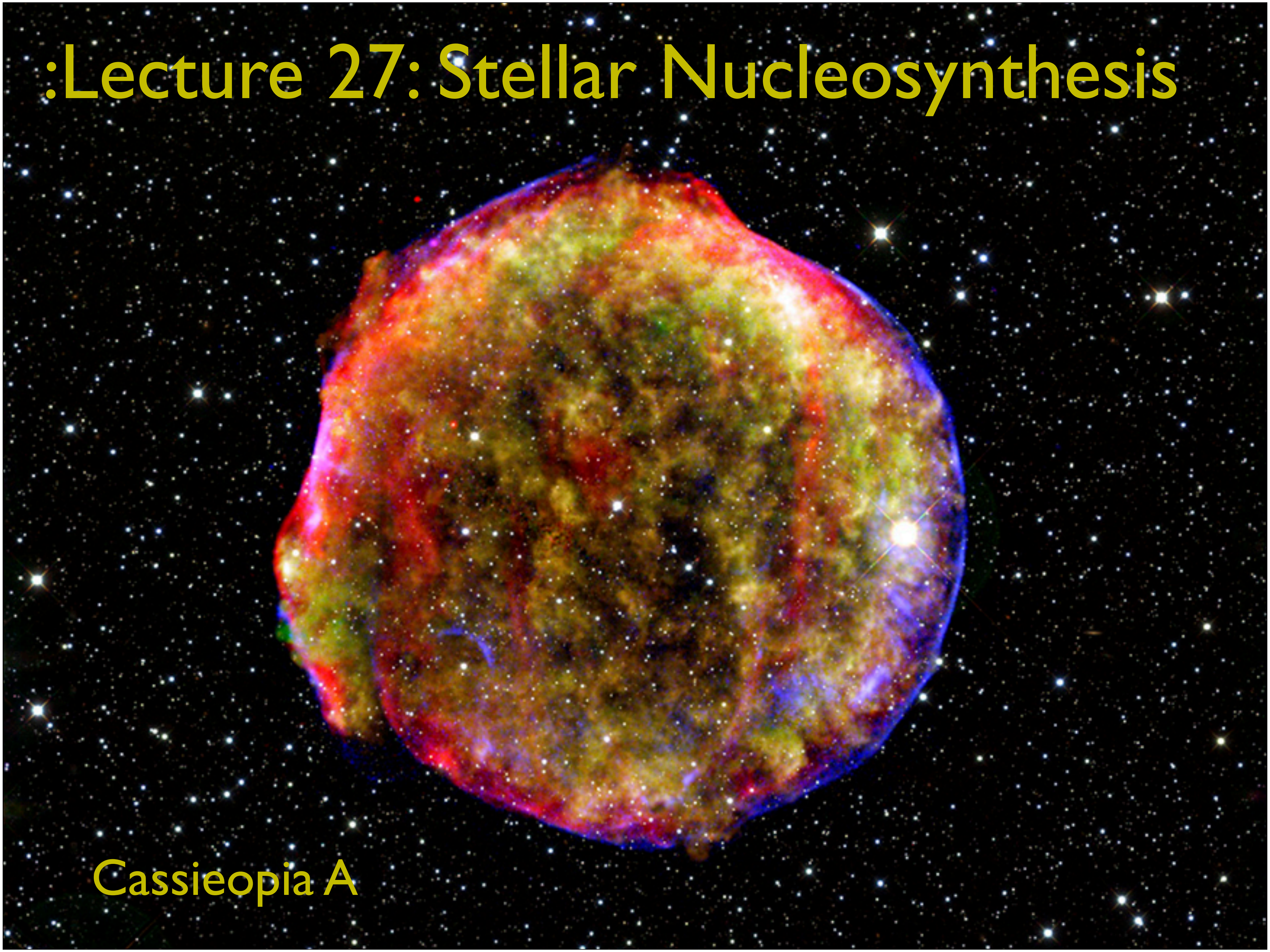

Cassieopia A

Major nuclear burning processes

Common feature is release of energy by consumption of nuclear fuel. Rates of energy release vary enormously. Nuclear processes can also absorb energy from radiation field, we shall see consequences can by catastrophic.

Nuclear Fuel	Process	$T_{threshold}$ 10^6K	Products	Energy per nucleon (Mev)
H	PP	~4	He	6.55
H	CNO	15	He	6.25
He	3α	100	C,O	0.61
C	C+C	600	O,Ne,Ma,Mg	0.54
O	O+O	1000	Mg,S,P,Si	~0.3
Si	Nuc eq.	3000	Co,Fe,Ni	<0.18

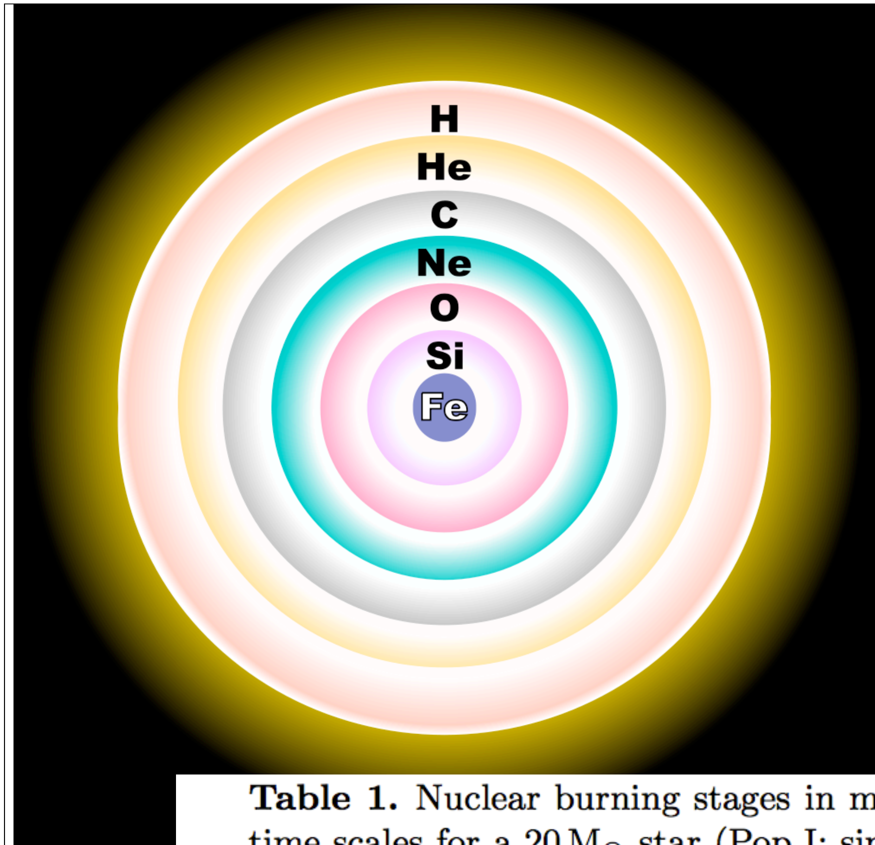

Table 1. Nuclear burning stages in massive stars. We give typical temperatures and time scales for a 20 $M_\odot$ star (Pop I; similar in Pop III) and a 200 $M_\odot$ star (Pop III)

Burning stages		20 $M_\odot$ star		200 $M_\odot$ star	
Fuel	Main product	T (10^9 K)	duration (yr)	T (10^9 K)	duration (yr)
H	He	0.037	8.1×10^6	0.14	2.2×10^6
He	O, C	0.19	1.2×10^6	0.24	2.5×10^5
C	Ne, Mg	0.87	9.8×10^2	$1.1^\dagger$	4.5
Ne	O, Mg	1.6	0.60	$2.4^\dagger$	1.1×10^{-6}
O	Si, S	2.0	1.3	$3.5^\dagger$	3.5×10^{-8}
Si	Fe	3.3	0.031	$4.3^\ddagger$	2.7×10^{-7}

†central radiative implosive burning ‡incomplete silicon burning at bounce

The Products from Burning

He^4 from hydrogen burning
He^3 from incomplete PP chain
D, Li, Be and B are bypassed
C^{12} and O^{16} from helium burning
O^{18} and Ne^{22} due to α capture by N^{14}
N^{14} from CNO conversion to N^{14}
Ne^{20}, Na, Mg, Al, Si^{28} from Carbon burning
Mg, Al, Si, P, S partly due to Oxygen burning

"Silicon Burning"

One might think the next step is

Si^{28} + Si^{28} => Ni^{56}

But this does not occur!

At this phase, photodisintegration becomes an important process.

Radiation is energetic enough to knock protons and α particles off of nuclei:

$$\lambda_\gamma \propto e^{-\frac{Q}{KT}}$$

Nuclear Statistical Equilibrium

Once photodisintegration starts, nuclei are continually gain and lose particles. Eventually, a statistical equilibrium is set up, which is similar to

$$\frac{N(A-1,Z)n_n}{N(A,Z)} = \frac{2G(A-1,Z)}{G(A,Z)} \frac{(2\pi\mu kT)^{3/2}}{H^3} e^{-\frac{Q}{KT}} \tag{13}$$

$$\frac{N(A-2,Z-1)n_p}{N(A-1,Z)} = \frac{2G(A-2,Z-1)}{G(A-1,Z)} \left(\frac{A-2}{A-1}\right)^{3/2} \frac{(2\pi\mu kT)^{3/2}}{H^3} e^{-\frac{Q}{KT}} \tag{14}$$

Non-equilibrium process is Beta decay (due to loss of Neutrinos)

Photodisintegration of Silicon

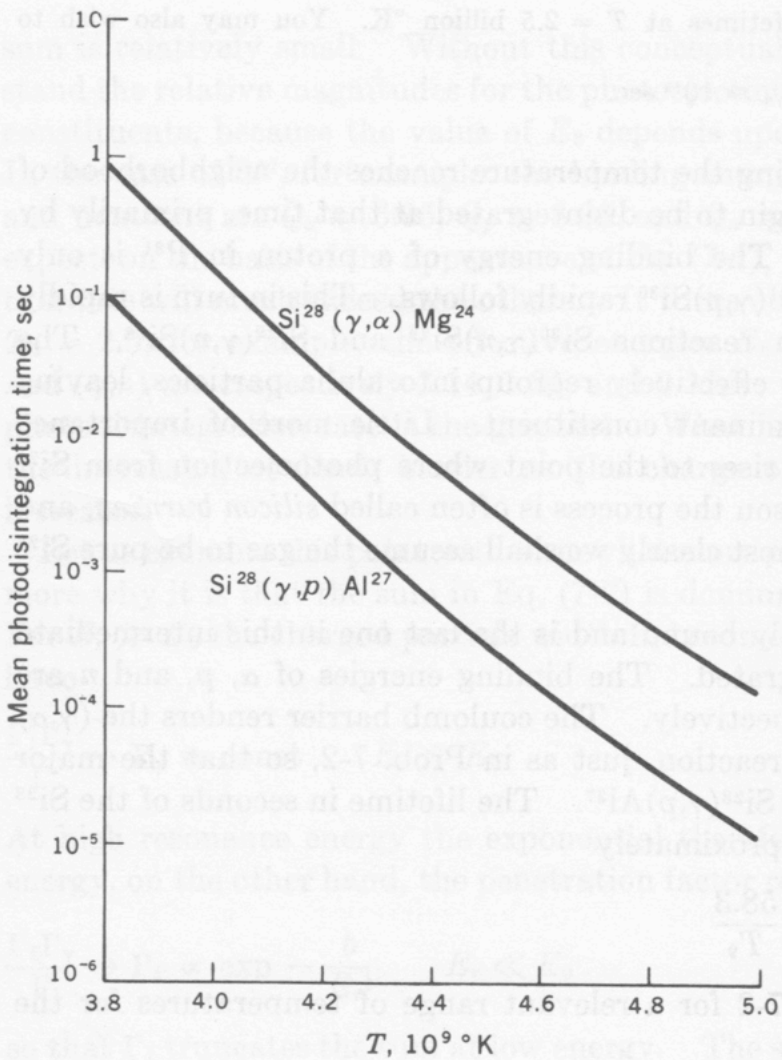

Fig. 7-2 The lifetime of the Si^{28} nucleus against photodisintegration. The lifetime has a strong temperature dependence, and the photoejection of protons is found to be somewhat faster than the photoejection of alpha particles. [*After J. W. Truran, A. G. W. Cameron, and A. A. Gilbert, Can. J. Phys.*, **44**:576 (1966).]

From Clayton: Principles of Stellar Evolution and Nucleosynthesis

Creation of New Elements due to Photodisintegration and Capture of Protons, Neutrons and α Particles

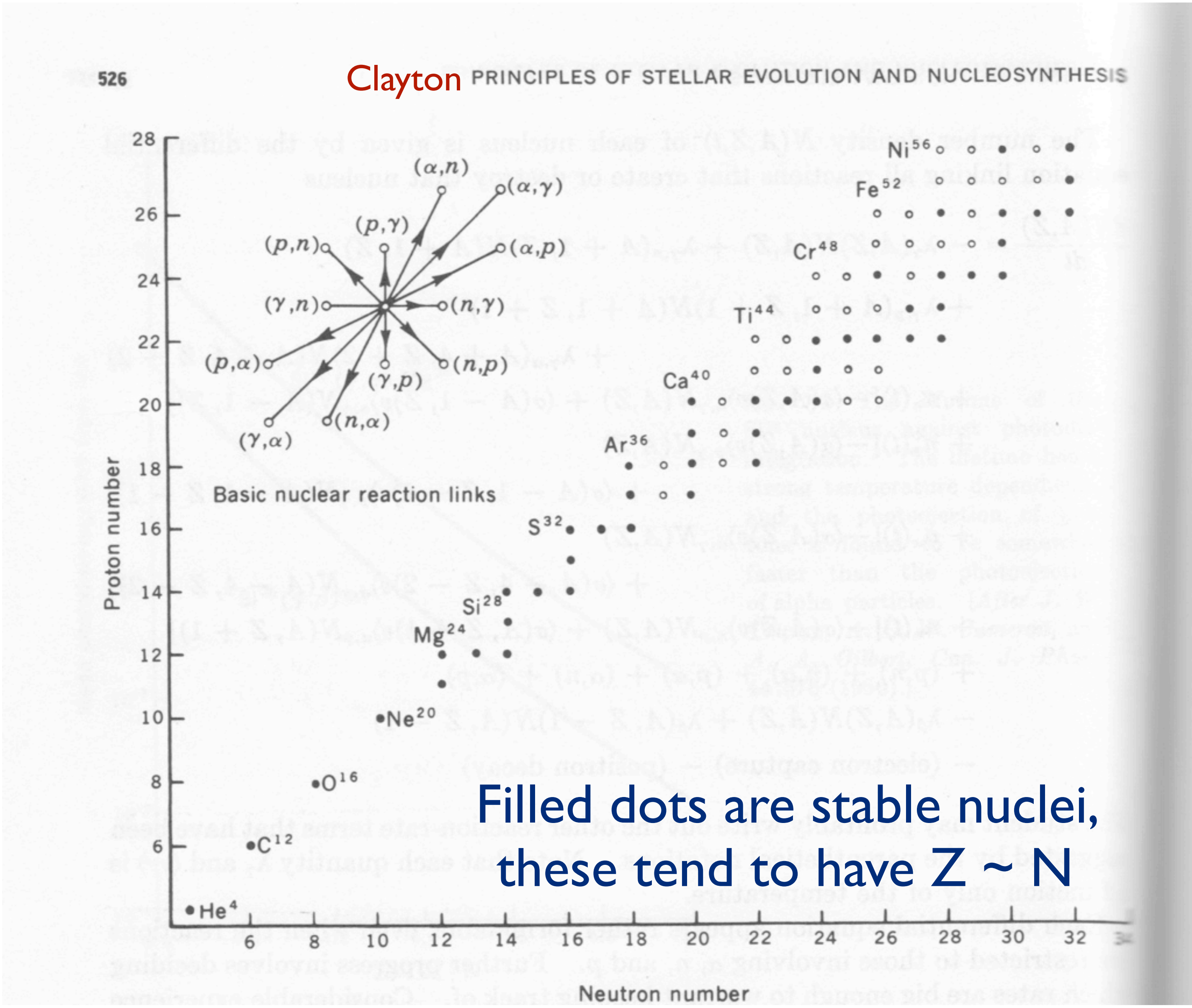

Filled dots are stable nuclei, these tend to have Z ~ N

Towards Nuclear Statistical Equilibrium

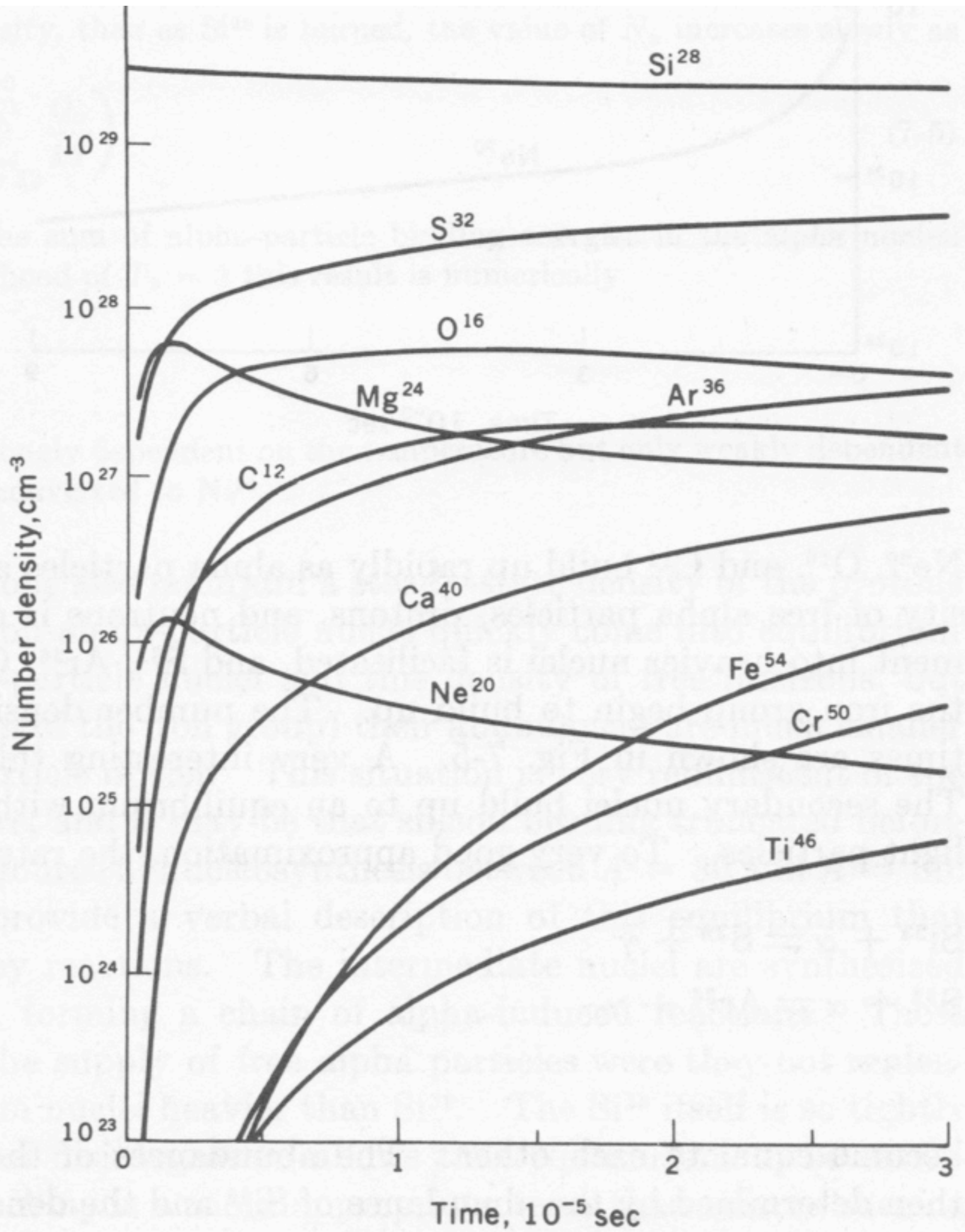

Fig. 7-4 The early phase of the nuclear rearrangement of initially pure Si^{28} at the temperature 5×10^9 °K and density 1.3×10^7 g/cm³. The abundances grow very rapidly at first, when the liberated alpha particles are being consumed in a rapid flow toward the iron group. [*After J. W. Truran, A. G. W. Cameron, and A. A. Gilbert, Can. J. Phys.*, **44**:576 (1966).]

Clayton

Dominant Elements in Nuclear Statistical Equilibrium

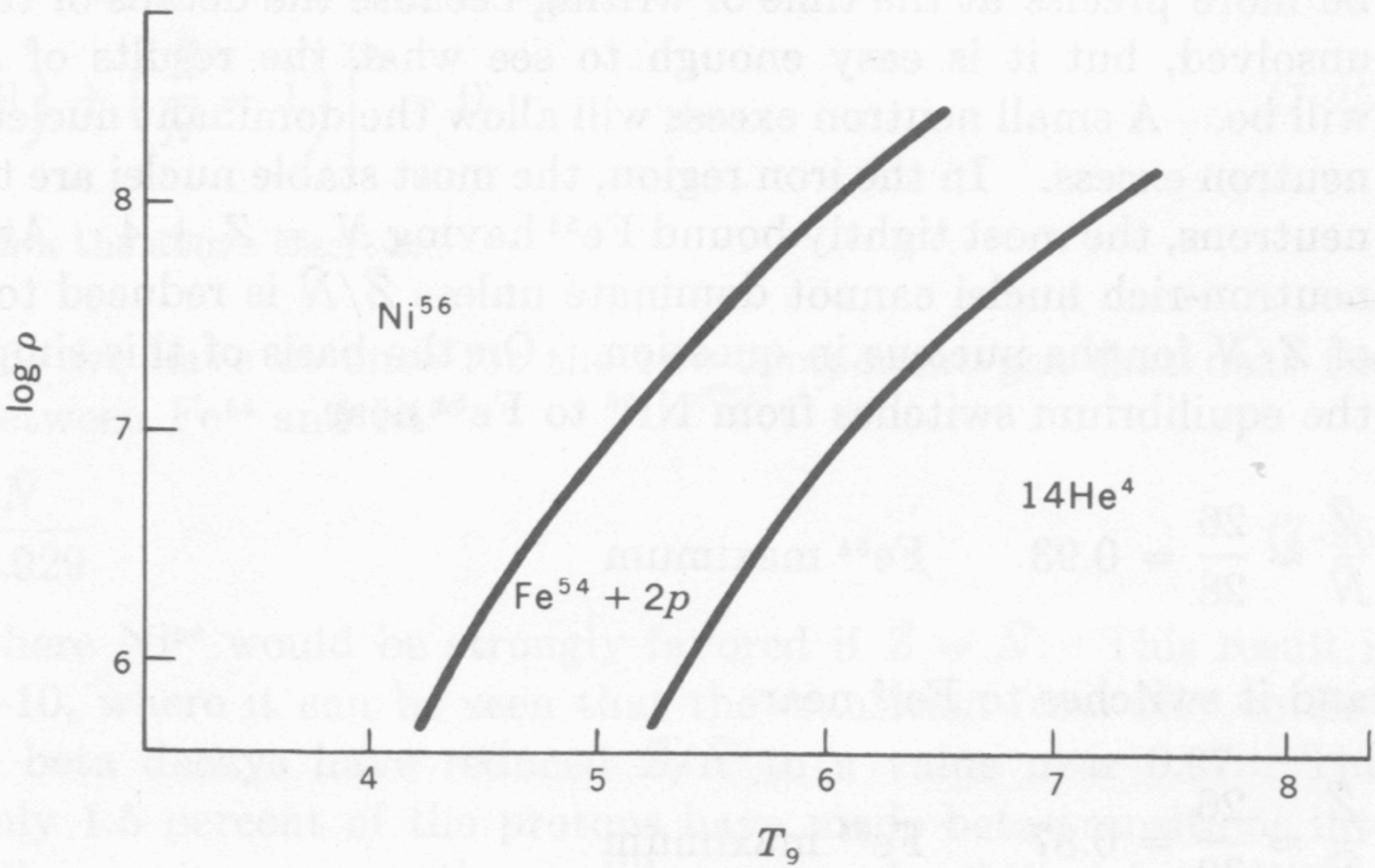

Fig. 7-9 The dominant nuclear constituent in a gas in nuclear statistical equilibrium when $\bar{Z}/\bar{N} = 1$.

Clayton

Dominant Elements in Nuclear Statistical Equilibrium

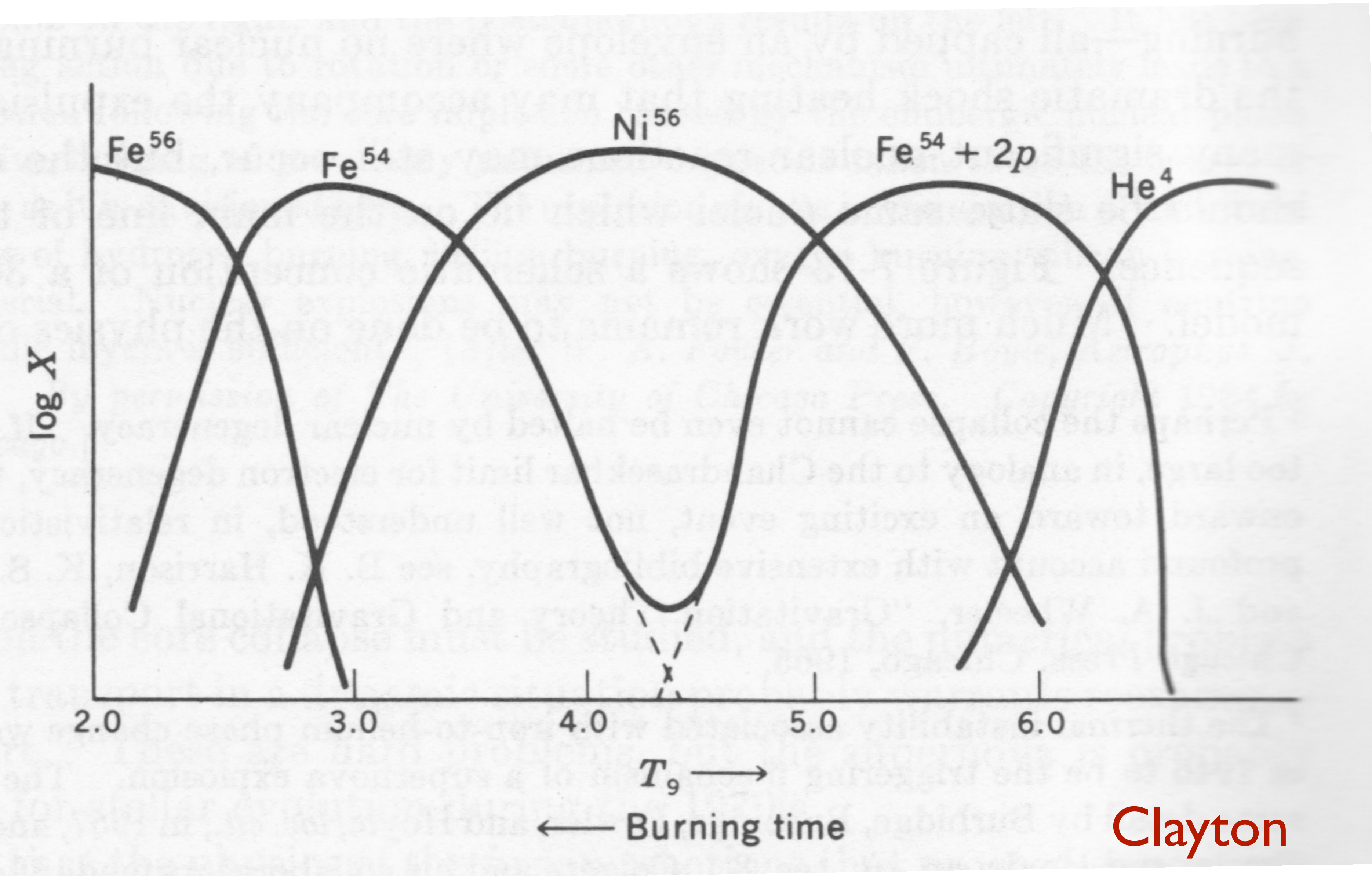

Clayton

Element Abundances Created in Nuclear Statistical Equilibrium (e burning)

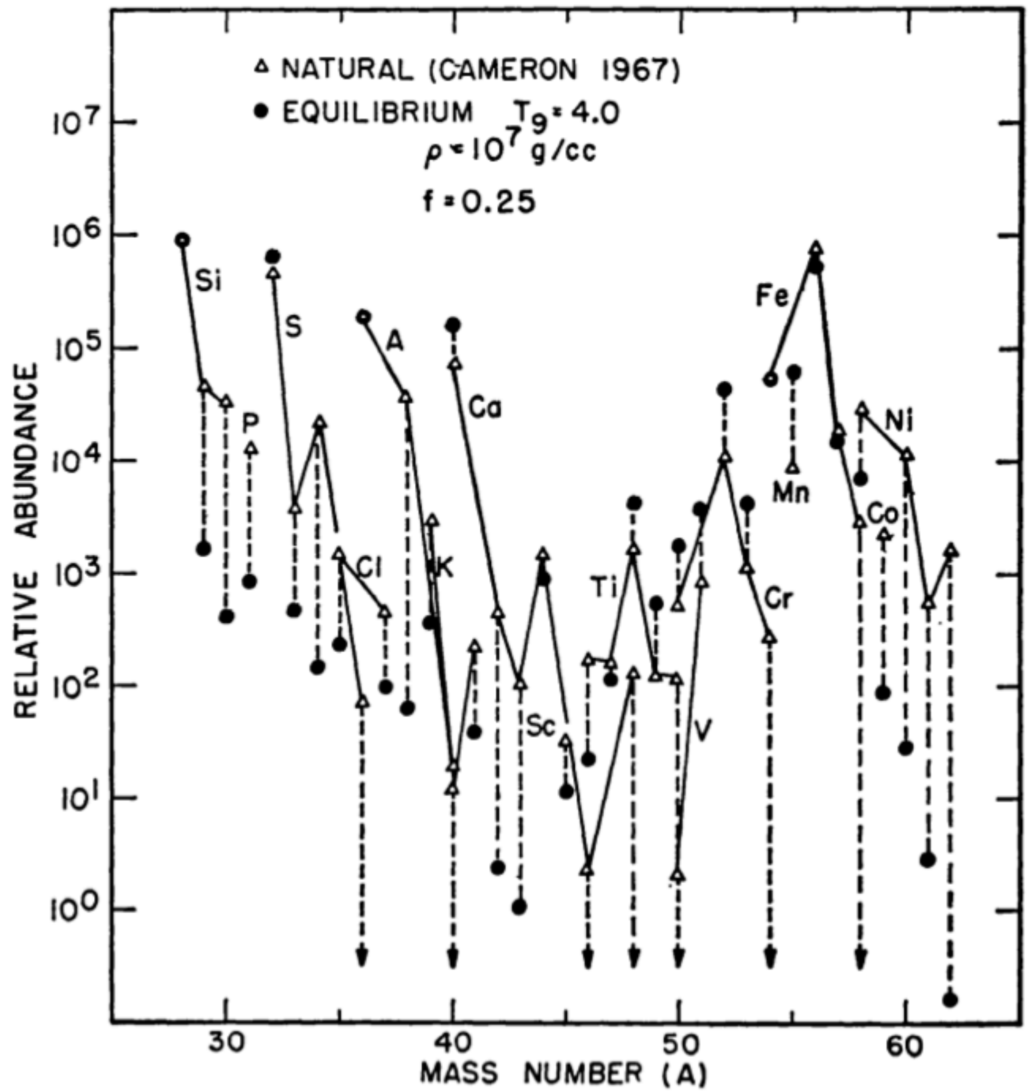

Bodansky, Clayton, & Fowler
Phys. Rev. Letter 1968

FIG. 21.—Comparison of natural solar-system abundances with quasi-equilibrium abundances at $T_9 = 4.0$, $\rho = 10^7$ gm cm^{-3}, and $f = 0.25$. The meteoritic iron abundance is used in this comparison.

Creating the Remainder of the Periodic Table

Neutrons: the r (rapid) and s (slow) processes

The Nuclear burning now creates enough neutrons that nuclei can grown through neutron capture.

Unlike Protons, Neutrons do not face Coloumb repulsion, thus elements with much larger values of Z can be produced.

In the process two types of reactions and two types of nuclei are involved:
Neutron captures and β-decays ; stable and unstable nuclei

Stable nuclei may undergo only neutron captures, unstable ones my undergo both, with the outcome depending on the timescales for the two processes.

What can we say about the timescales of these processes ?

Hence neutron capture reactions may proceed more ***slowly*** or more ***rapidly*** than the competing β-decays. The different chains of reactions and products are called the ***s-process*** and ***r-process***.

Formation of Cobalt from Neutron Capture

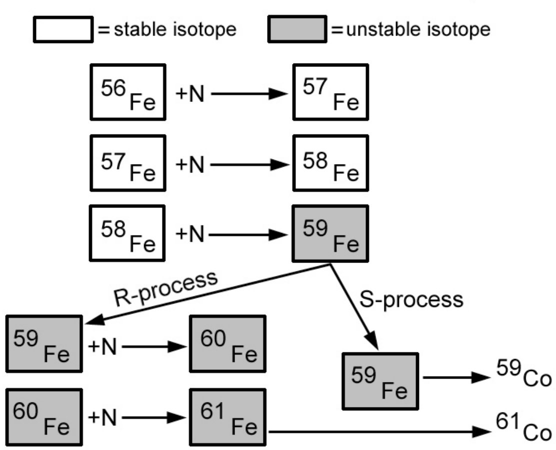

R Process

Rapid neutron capture

$$^{65}Cu + 5n \Rightarrow {}^{70}Zn + \beta^- + \nu + Q$$

Slide: Stephen Smartt

Some basic examples

R Process

Rapid neutron capture

$$^{65}Cu + 5n \Rightarrow {}^{70}Zn + \beta^- + \nu + Q$$

S Process

$$^{62}Ni + n \Rightarrow {}^{63}Ni + \gamma + Q$$

$$^{63}Ni \Rightarrow {}^{63}Cu + \beta^- + \nu + Q$$

$$^{63}Cu + n \Rightarrow {}^{64}Cu + \gamma + Q$$

Branched Decay

$$^{64}Cu \Rightarrow {}^{64}Zn + \beta^- + \nu + Q$$

$$^{64}Cu \Rightarrow {}^{64}Ni + \beta^+ + \nu + Q$$

$\Rightarrow$

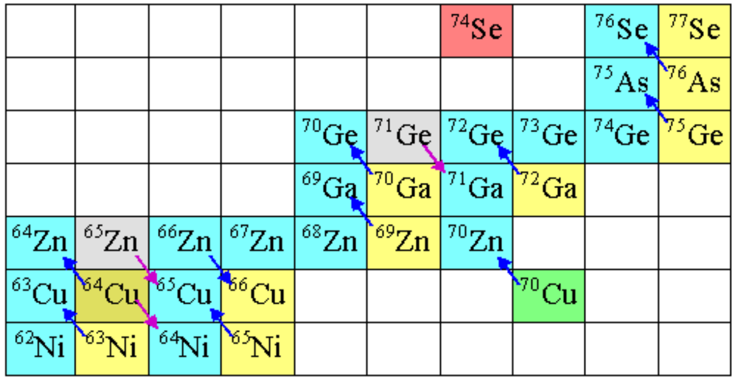

Simple explanation of *r* and *s* process on:
ultraman.ssl.berkeley.edu/nucleosynthesis.html

Slide: Stephen Smartt

Elemental Abundances in the Solar System

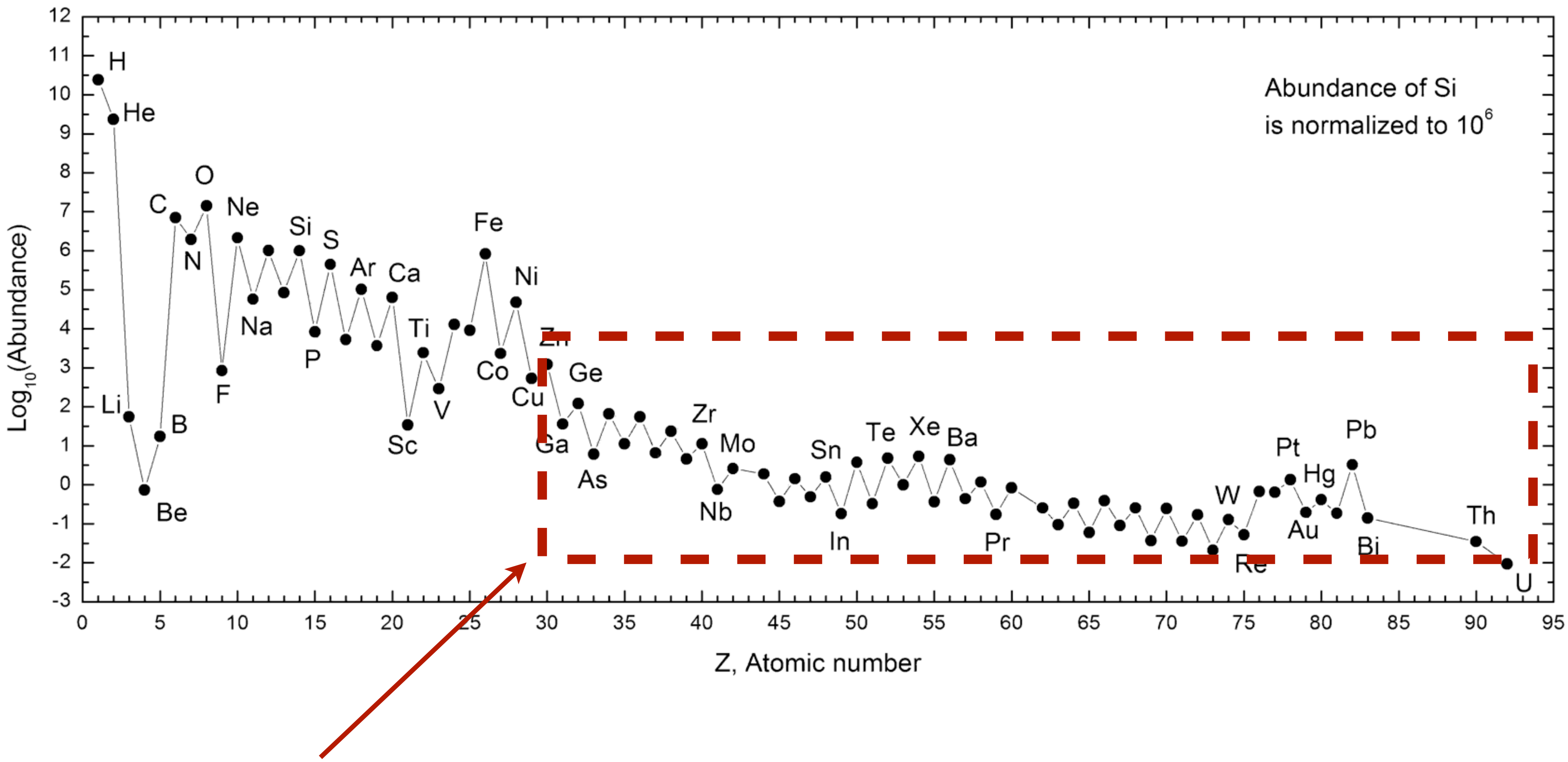

Synthesized by S and R-processes

What causes all the structure?

the s-process

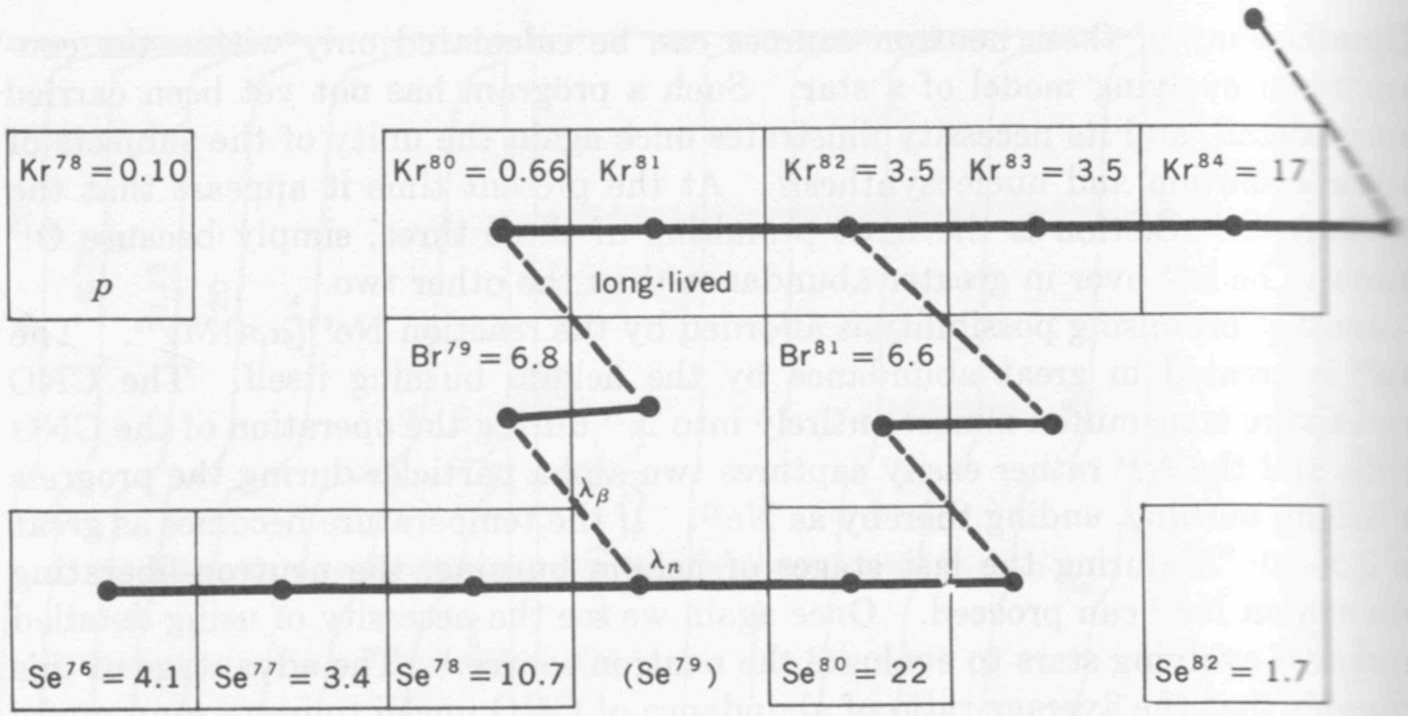

Fig. 7-26 The *s*-process path through selenium, bromine, and krypton. An interesting branch between neutron capture and beta decay occurs at Se^{79}, which has a laboratory half-life of 6.5×10^4 years. Both Kr^{80} and Kr^{82} are shielded from *r*-process production, by Se^{80} and Se^{82}, respectively. The ratio of *s*-process current through Kr^{80} to that through Kr^{82} is equal to the ratio of $\lambda_\beta(Se^{79})$ to $\lambda_\beta(Se^{79}) + \lambda_n(Se^{79})$. The abundance of each nucleus per 10^6 silicon atoms in the solar system is indicated.

The s-processes produces stable nuclei where Z ~ N

Cross Section to Neutron Capture

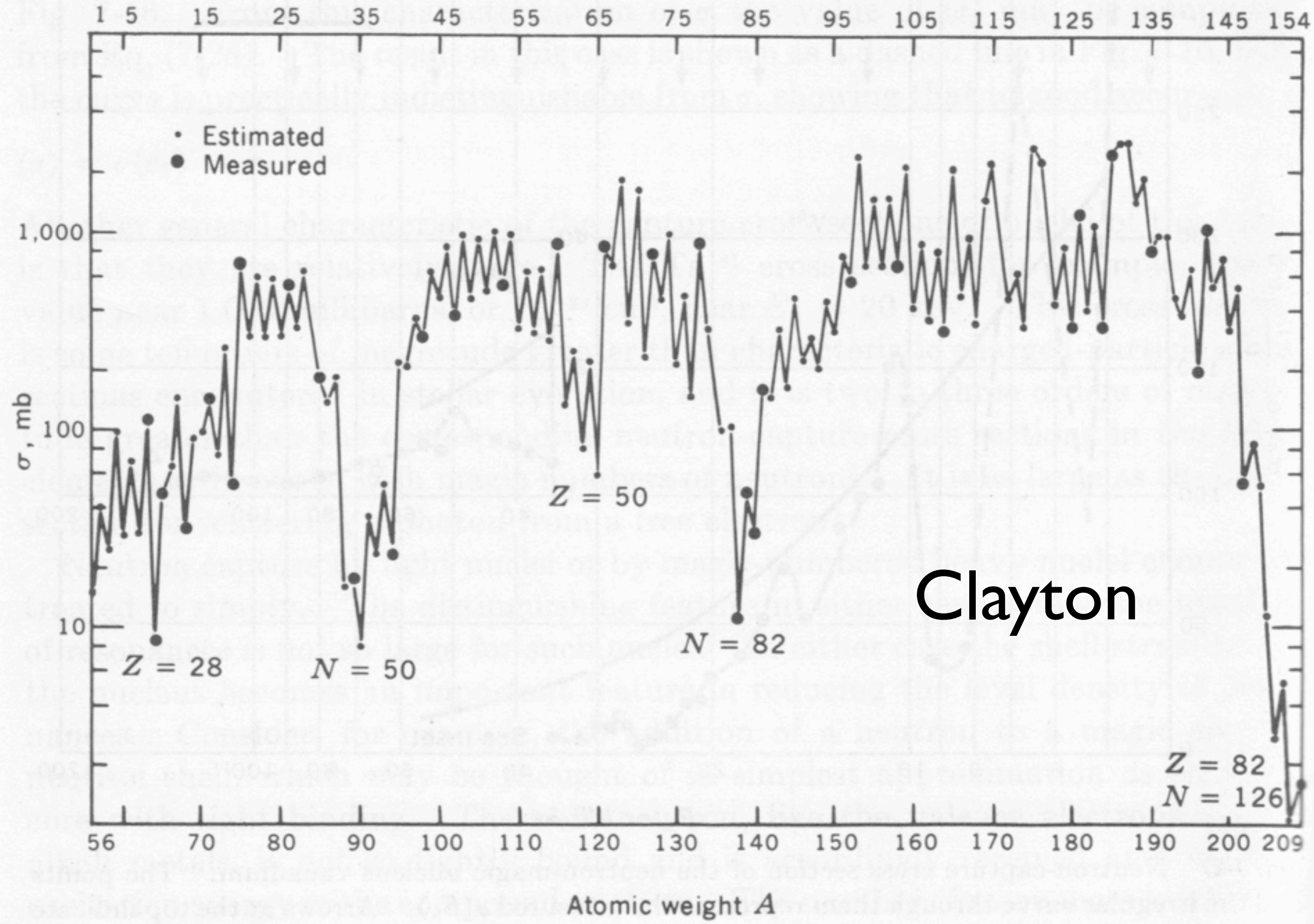

Clayton

Fig. 7-18 Measured and estimated neutron-capture cross sections of nuclei on the *s*-process path. The neutron energy is near 25 kev. The cross sections show a strong odd-even effect reflecting average level densities in the compound nucleus. Even more obvious is the strong influence of the closed nuclear shells, or magic numbers, which are associated with precipitous drops in the cross section. Nucleosynthesis of the *s*-process nuclei is dominated by the small cross sections of the neutron-magic nuclei.

s-process abundances

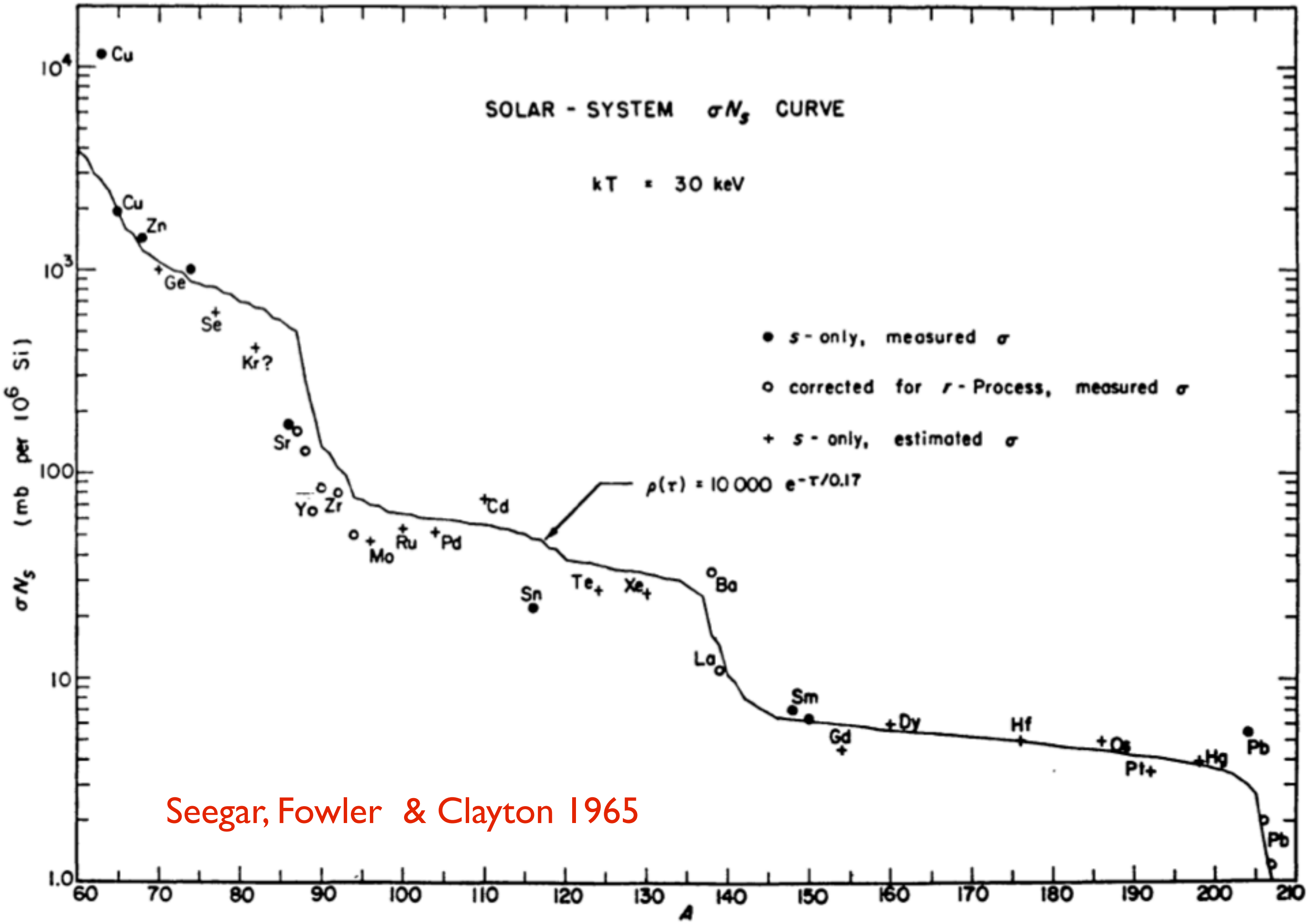

FIG. 1.—Solar-system σN_s-curve. The product of the neutron-capture cross-section at $kT = 30$ keV (in mb) times isotopic abundance (Si = 10^6) is plotted versus atomic mass number A. The solid line is a calculated curve corresponding to an exponential distribution of integrated neutron flux.

The points are the neutron cross-section x the solar system abundance. This varies smoothly with atomic weight. The line is the theoretical prediction calculated assuming an exponential distribution of neutron exposures.

the s and r-processes

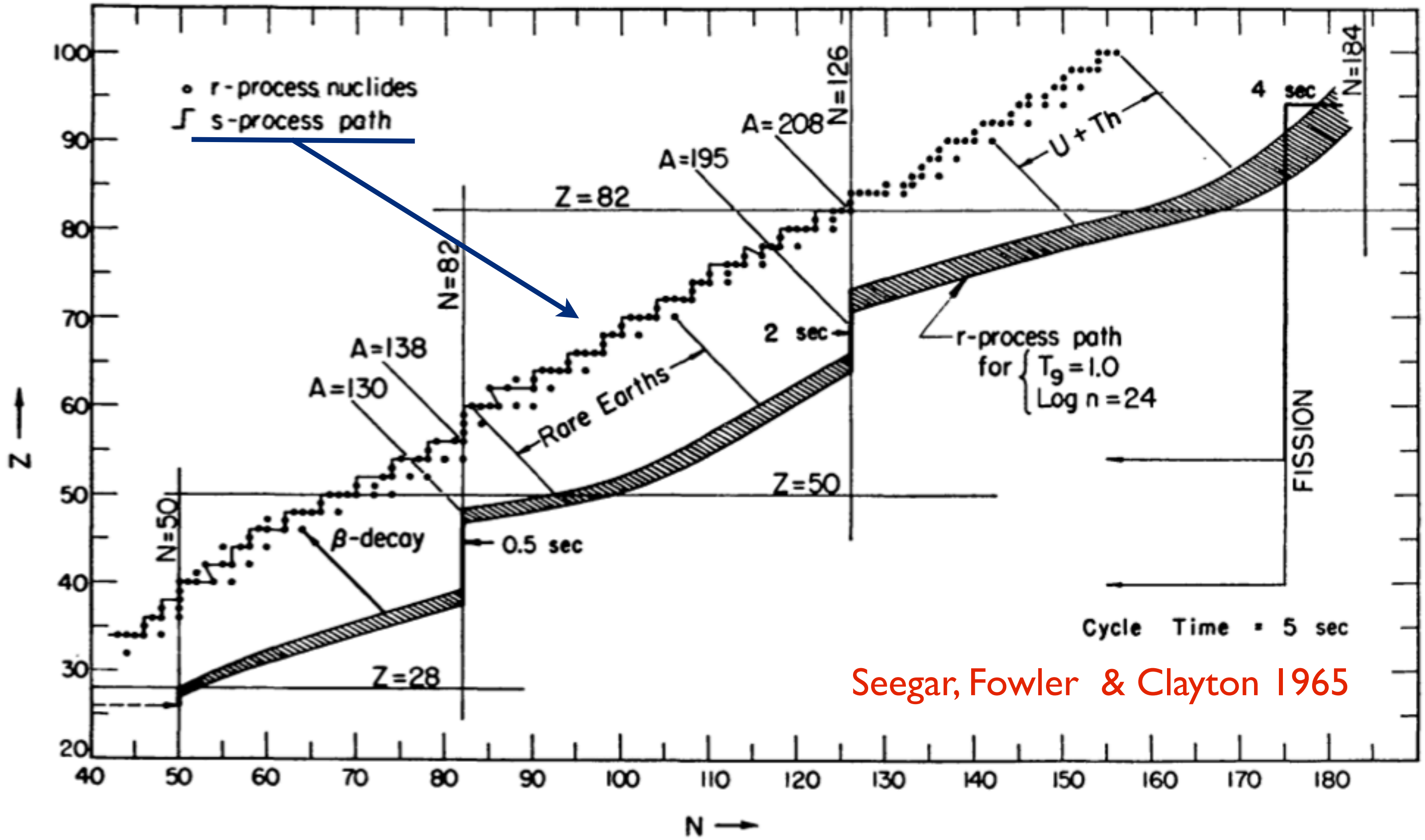

FIG. 10.—Neutron-capture paths. The *s*-process follows a path in the *N*–*Z*-plane which is near the line of beta-stability, and is represented by the single line. The *r*-process progenitor nuclei occupy a band in the neutron-rich area of the *N*–*Z*-plane, such as the shaded area here (calculated for $T_9 = 1.0$, log $n_n = 24$). Subsequently the progenitors beta-decay to the stable nuclei represented by circles; in many cases these end products of the *r*-process are also produced in the *s*-process. The observed abun dance peaks at $A = 130$ and $A = 138$ are attributed to the magic neutron number 82, and the peaks at $A = 195$ and $A = 208$ to $N = 126$. As neutrons are captured in the *r*-process, material starting at $Z = 26$ in the lower left-hand corner moves up the shaded band, reaching the $A \sim 130$ peak 0.5 sec and the $A \sim 195$ peak 2 sec after starting. After 4 sec material begins to reach $Z = 94$, where neutron-induced fission occurs; then a cyclic situation is established, and the number of nuclei is doubled by fission every 5 sec.

the r-process elements

SYNTHESIS OF THE HEAVY ELEMENTS 561

Clayton

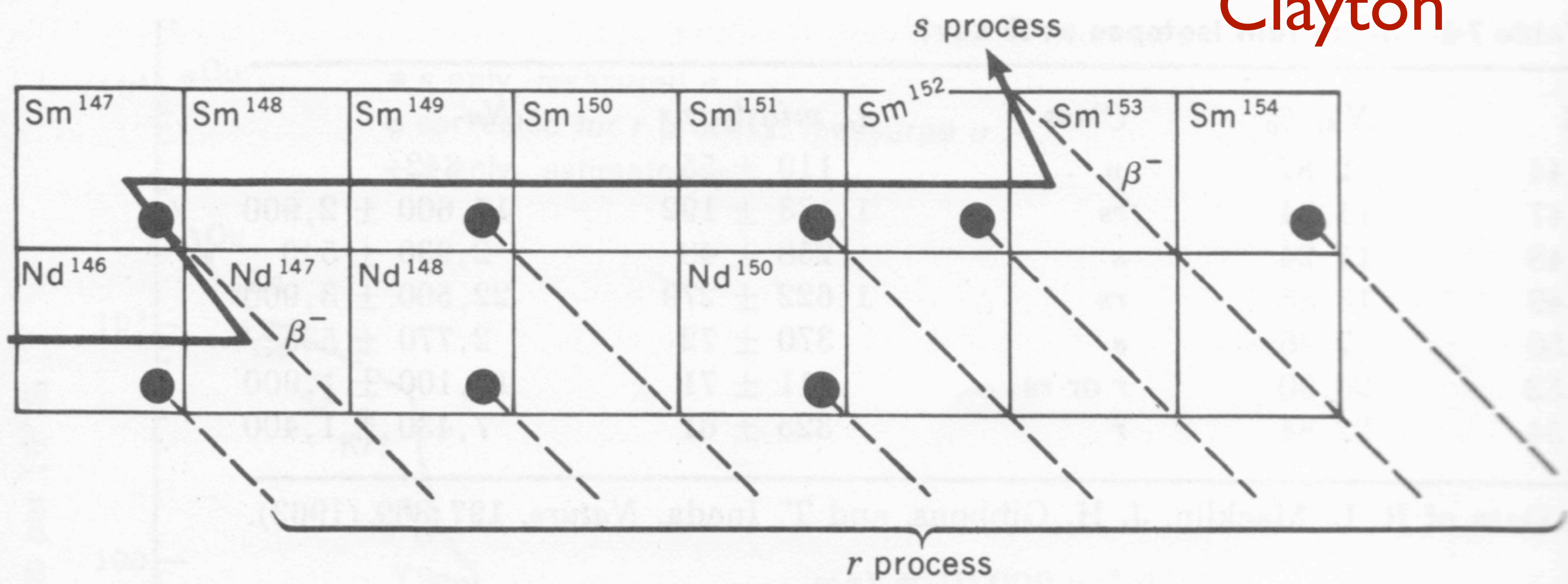

Fig. 7-19 The *s*-process path through the isotopes of samarium. The *r*-process yield contributes to the abundances of the nuclei containing the solid dots. Two of the isotopes of samarium, Sm^{148} and Sm^{150}, are *s*-only nuclei.

The r-process elements are created when the neutron rich elements undergo beta decay.

the r-process

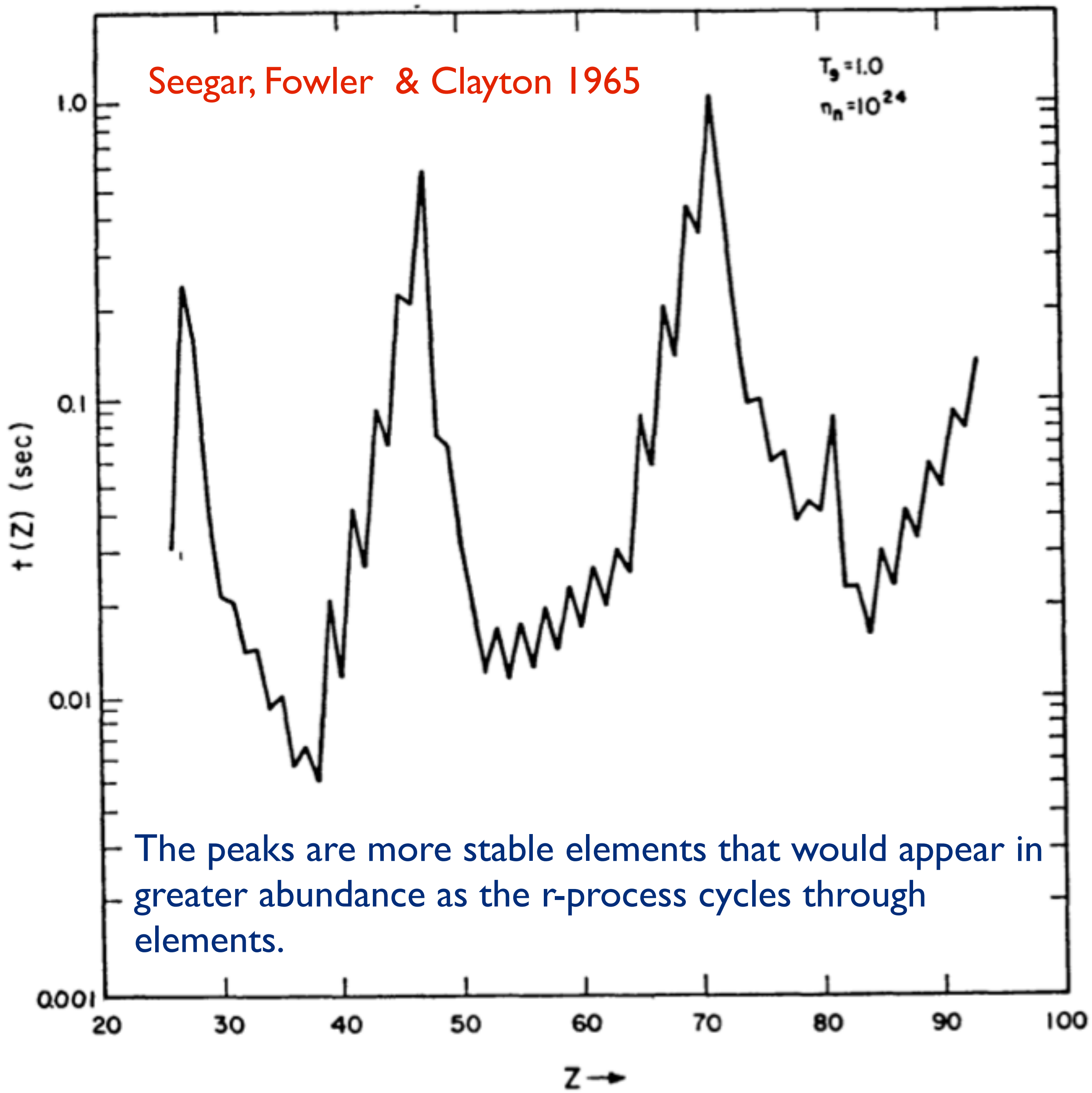

FIG. 11.—Beta-decay mean life. The mean life for beta-decay of the isotopes of each Z is plotted versus Z.

the r-process predicted abundances

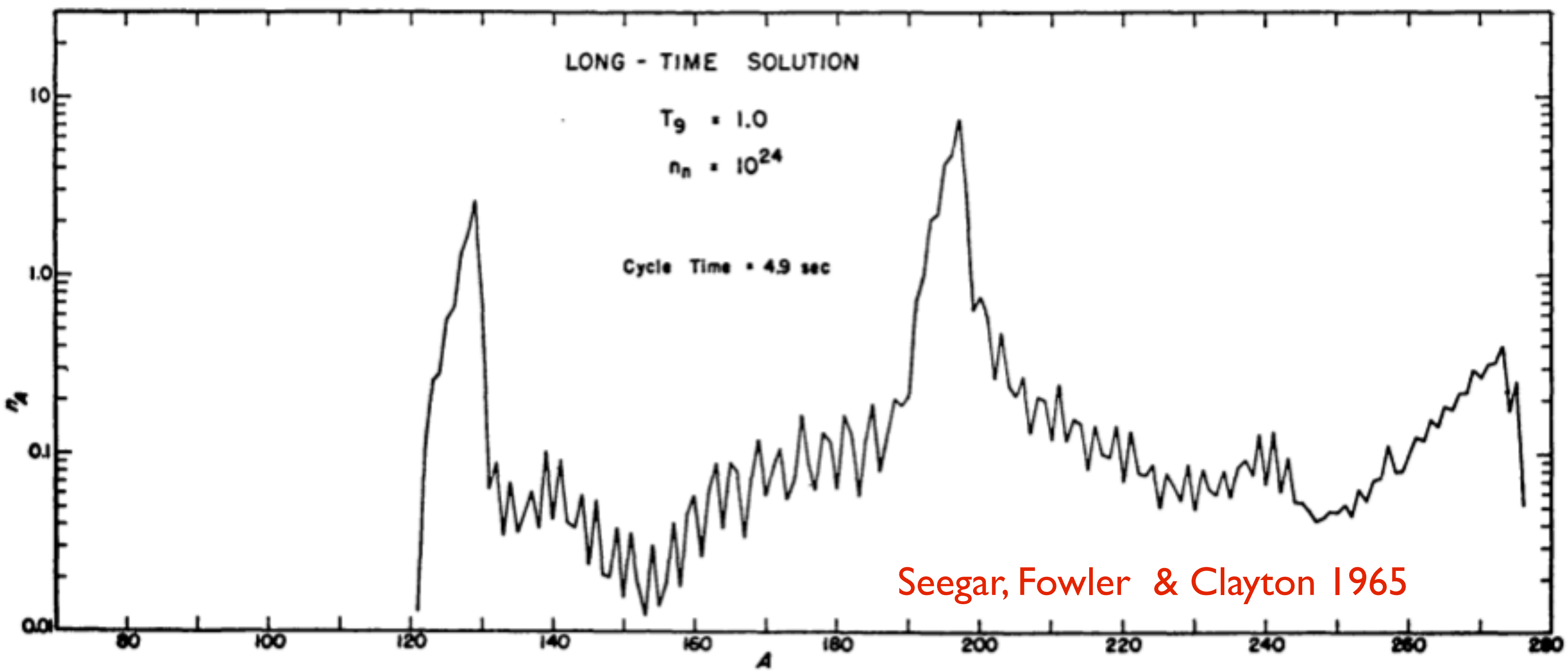

FIG. 13

As the r-process cycles through the elements (every 5 seconds in the above models), the above abundance distribution will be established. The abundances will double every cycle. Peaks are due to stable nuclei.

r-process abundances

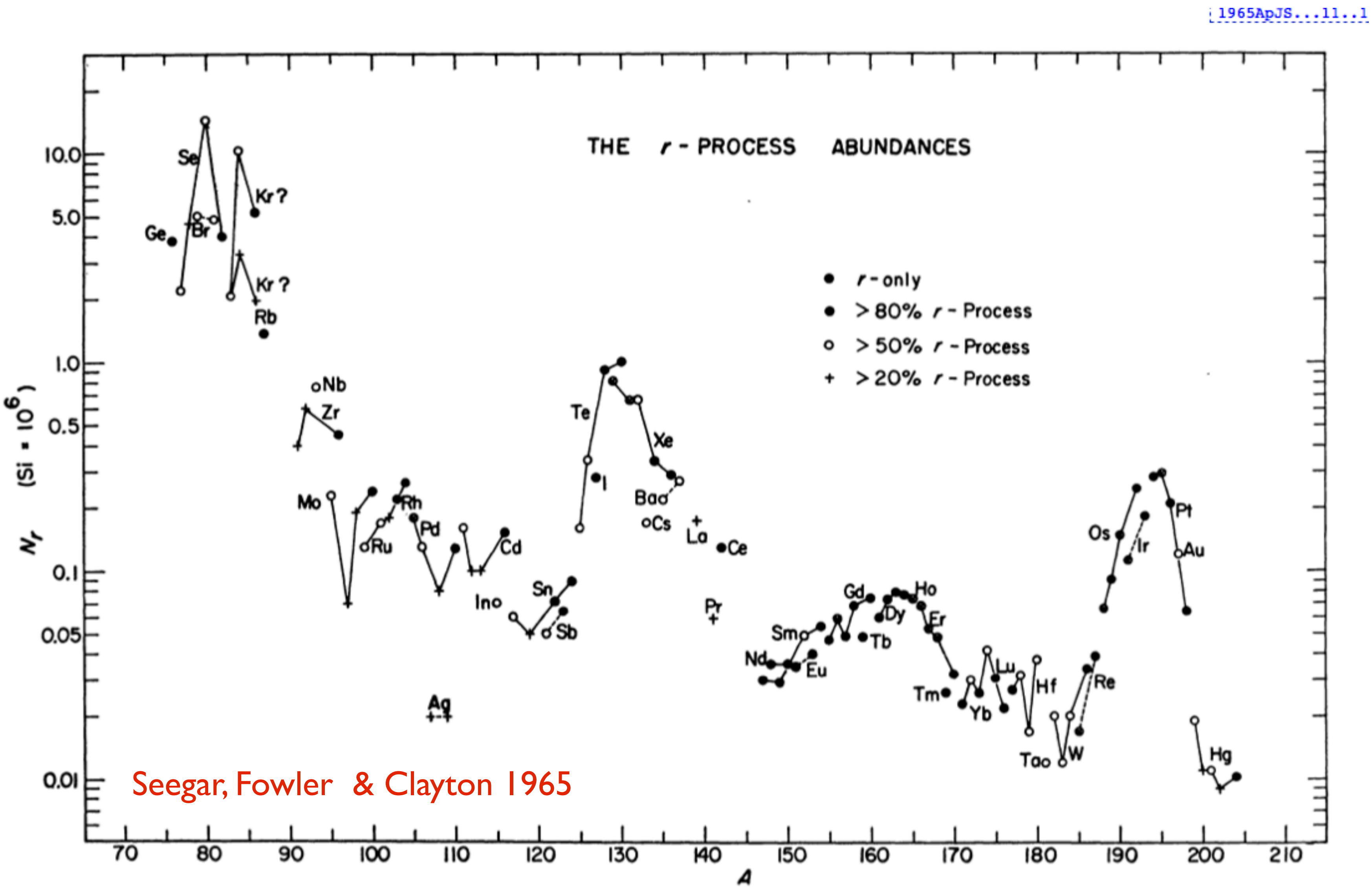

FIG. 6.—Solar-system r-process abundances. Abundances of isotopes produced in the r-process are plotted after subtraction of the contribution by the s-process. Isotopes of a given element are joined by lines (solid line = even Z, dashed line = odd Z). The ambiguity at Kr is discussed in the text.

These are R-process abundances after the subtraction of the S-process abundances

Density of Neutrons for R and S Processes

$$n_n = 10^5 \text{ cm}^{-3} \text{ for S process}$$

$$n_n = 10^{23} \text{ cm}^{-3} \text{ for R process}$$

An important question is where do the neutrons come from?

S-process may come from Carbon and Oxygen burning and the subsequent photodisitengration at even higher temperature. There may be some neutron production by side reactions during Helium burning - for example $^{13}C(\alpha,n)^{16}O$ (i.e. $^{13}C + \alpha \Rightarrow ^{16}O + n$).

R-process may require a supernova.

Evidence for Nucleosynthesis

Technetium

Tc Z = 43

Half life: ^{98}Tc = 4.2×10^{6} yr

^{99}Tc = 2×10^{5} yr

c: complex;   w: wide

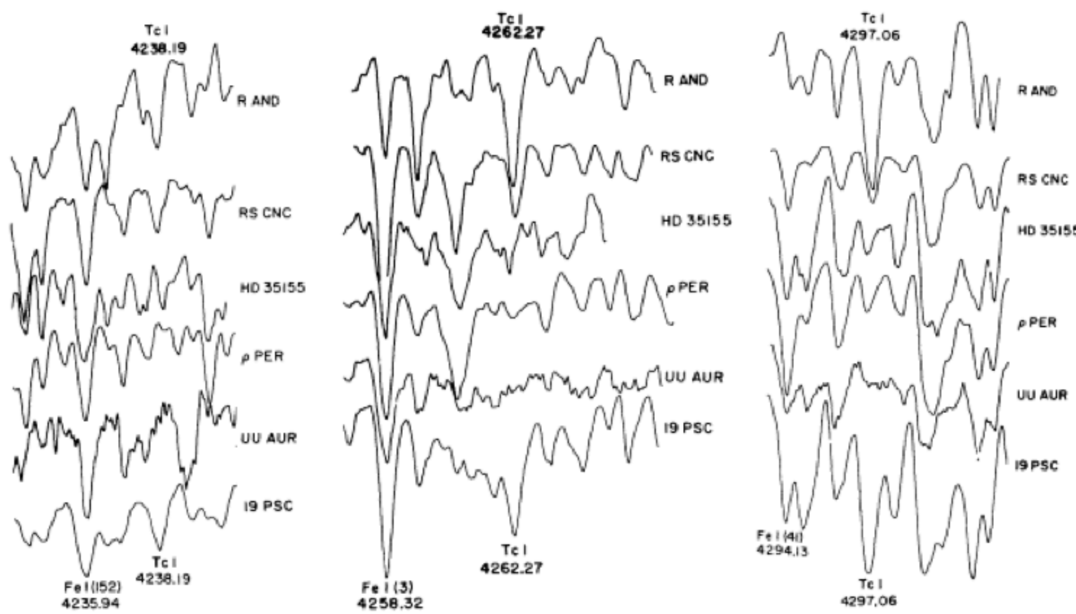

Fig. 1 — Microphotometer tracings of various Tc stars in the regions of the three zero-volt Tc lines: R And (S6, 6e; LPV), RS Cnc (M6S; irregular), HD 35155 (S4, 1; nonvariable), ρ Per (M4 II–III, shown for comparison), UU Aur (N3; C5, 5; semiregular), 19 (TX) Psc (N0; C6, 2; irregular).

Peary 1971

Found in Mira variables with P > 300 day (low mass stars undergoing AGB pulsations)

Technetium can be produced by s-process

Little-Marenin 1989

Path of s-process through Tc Region

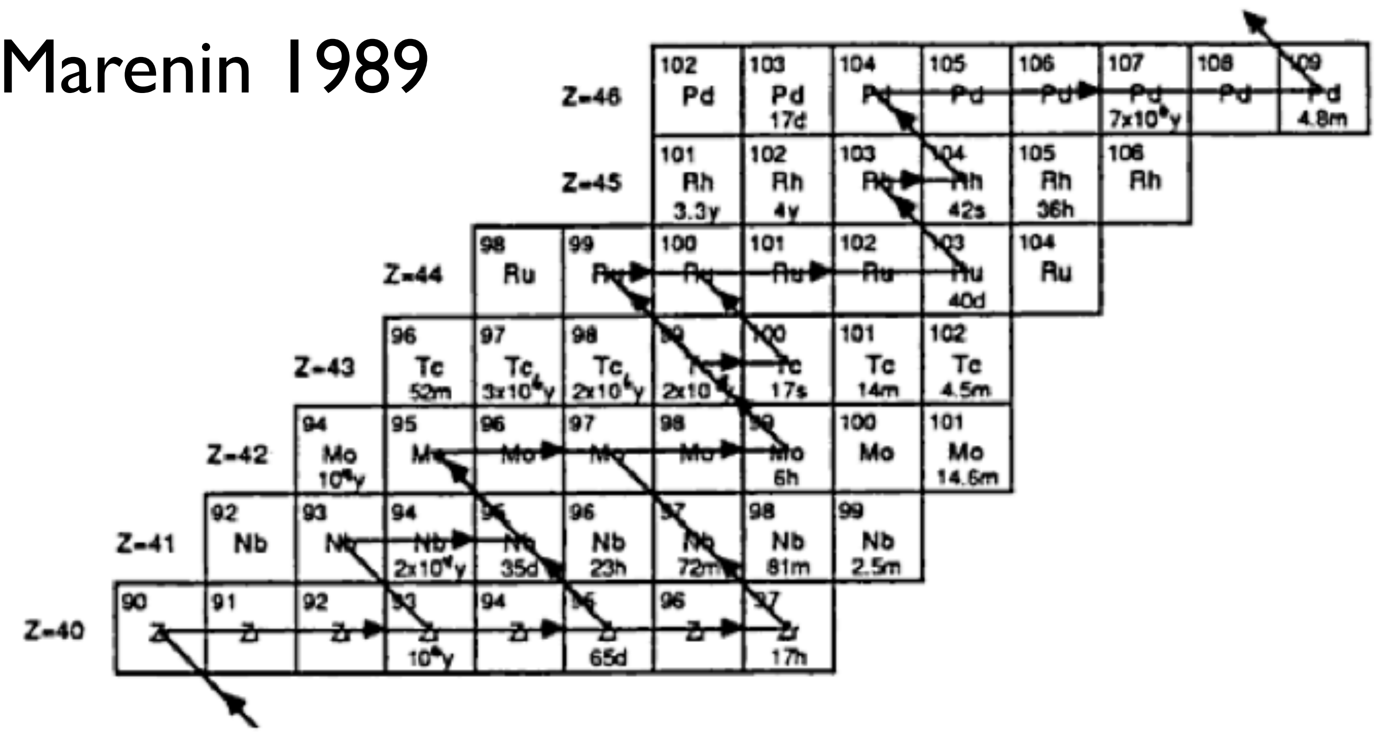

Figure 1 illustrates the s-process path in the Tc regions. The half-lives are listed for the radioactive isotopes of each element.

AGB stars can support S process

Supernova may be needed for R process

The Destruction of Lithium in Young Convective Stars

The ISM contains Lithium, 10% of which is primordial Lithium created in the Big Bang and the other 90% was created by future generations of stars. This Lithium is incorporated into the star during star formation.

The abundance is very low: $^{7}Li/H \sim 10^{-9}$

During Pre-main sequence evolution, Lithium can be destroyed by nuclear reactions.

For example: $p + {}^{7}Li \Rightarrow {}^{4}He + {}^{4}He$

The temperature required is a ~ 3×10^{6} K for ^{7}Li, and at lower temperatures for ^{6}Li - so this can happen before the onset of Hydrogen burning.

Because of the low abundance of Lithium, this cannot supply enough energy to halt pre-main sequence evolution.

This is part of the PPII chain, however, it happens here not with Lithium created by nuclear burning, but by using "primordial" Lithium.

In a low mass, convective star, the onset of Lithium burning will deplete Lithium throughout the entire star. The reason is that convection carries Lithium to the core, and Lithium depleted gas from the core.

Stars with radiative zones will not show Li depletion. Brown dwarfs will also not show Lithium depletion due to low temperatures in cores at the onset of degeneracy.

In these plots, stars evolve upward toward older ages and higher core temperatures.

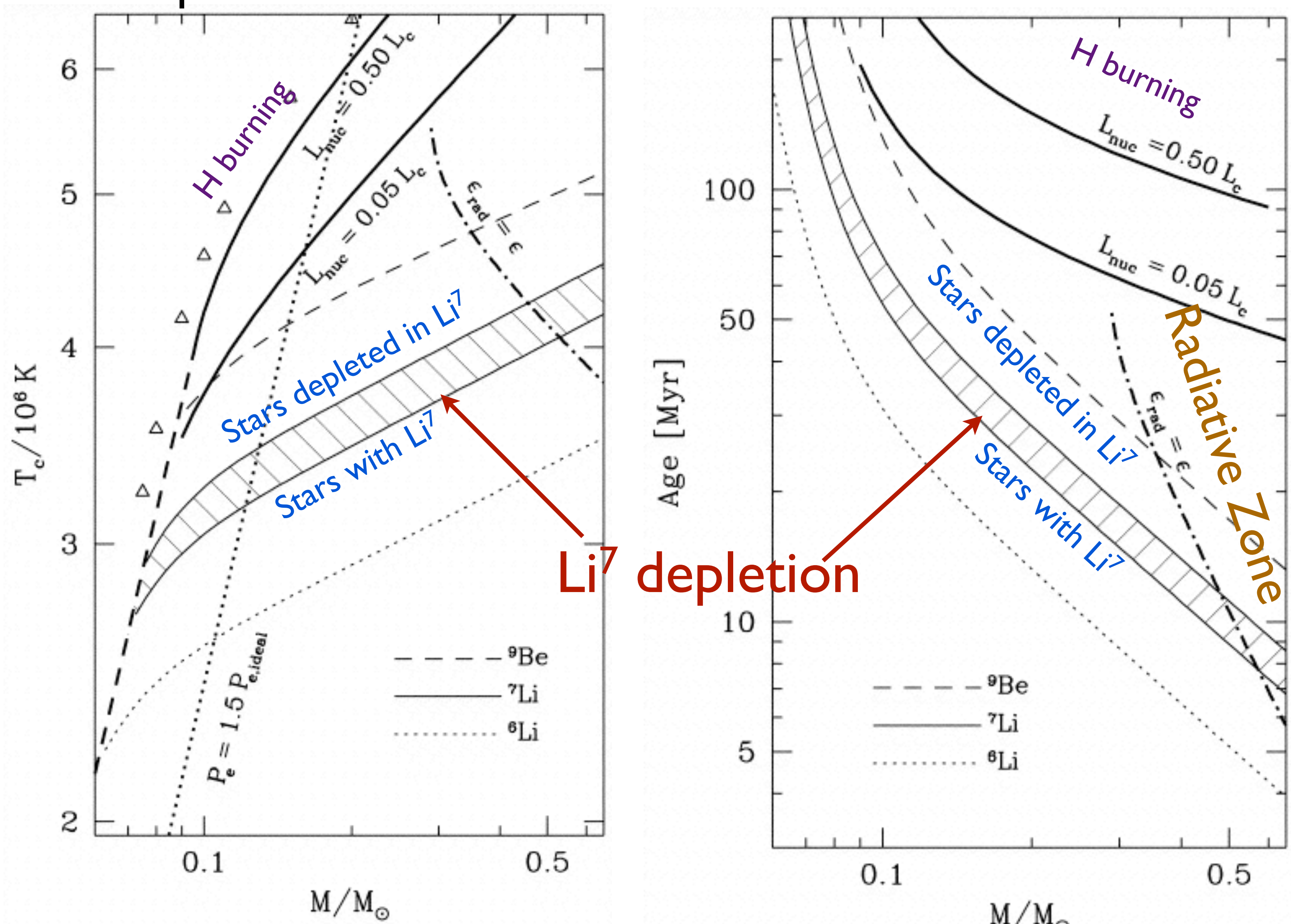

Ushomirsky 1998 Also see: http://online.kitp.ucsb.edu/online/astrot00/bildsten/

Star with Lithium in α Persei cluster (Stauffer et al. 1999)

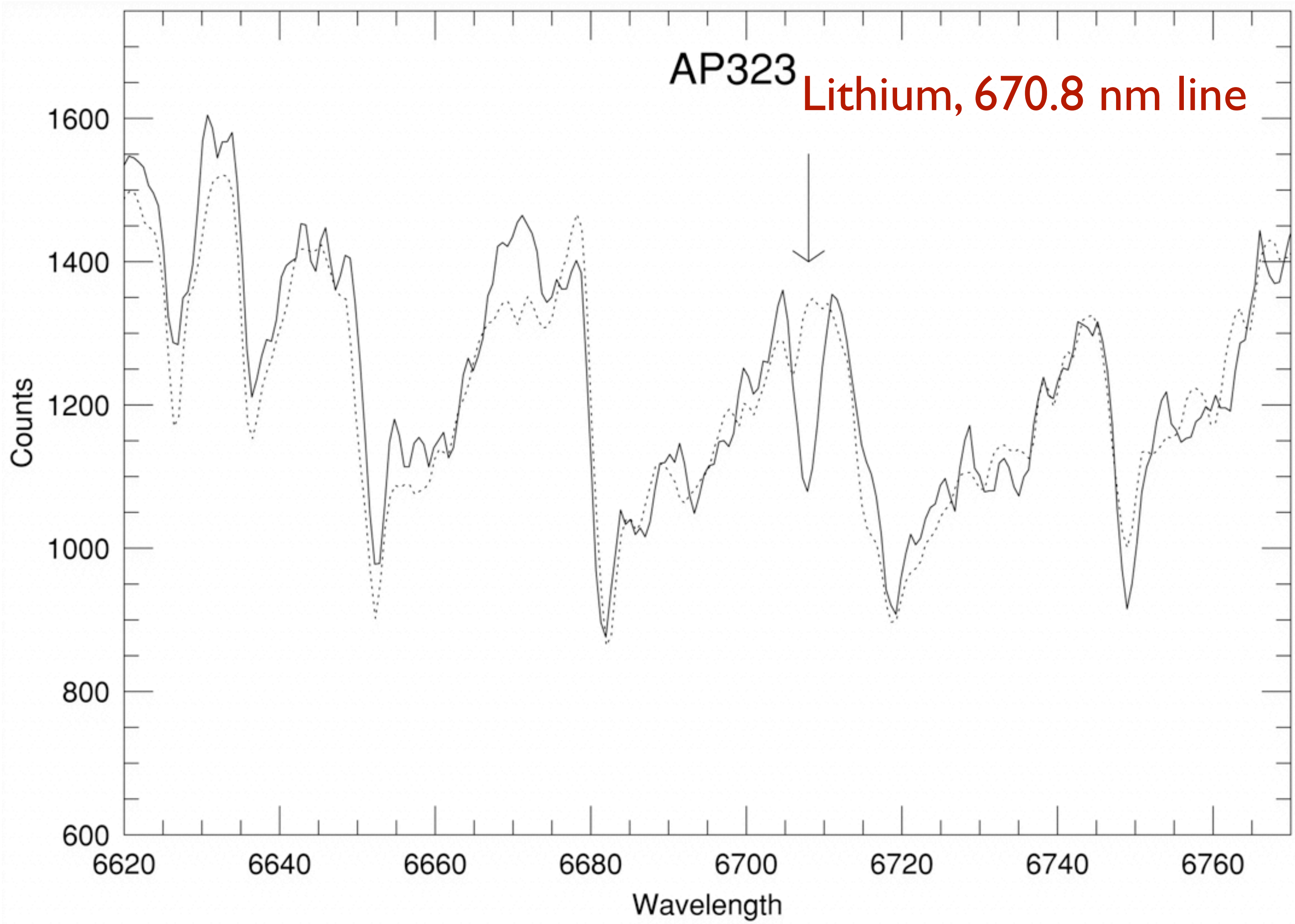

Lithium Depletion in α Persei cluster (Stauffer et al. 1999)

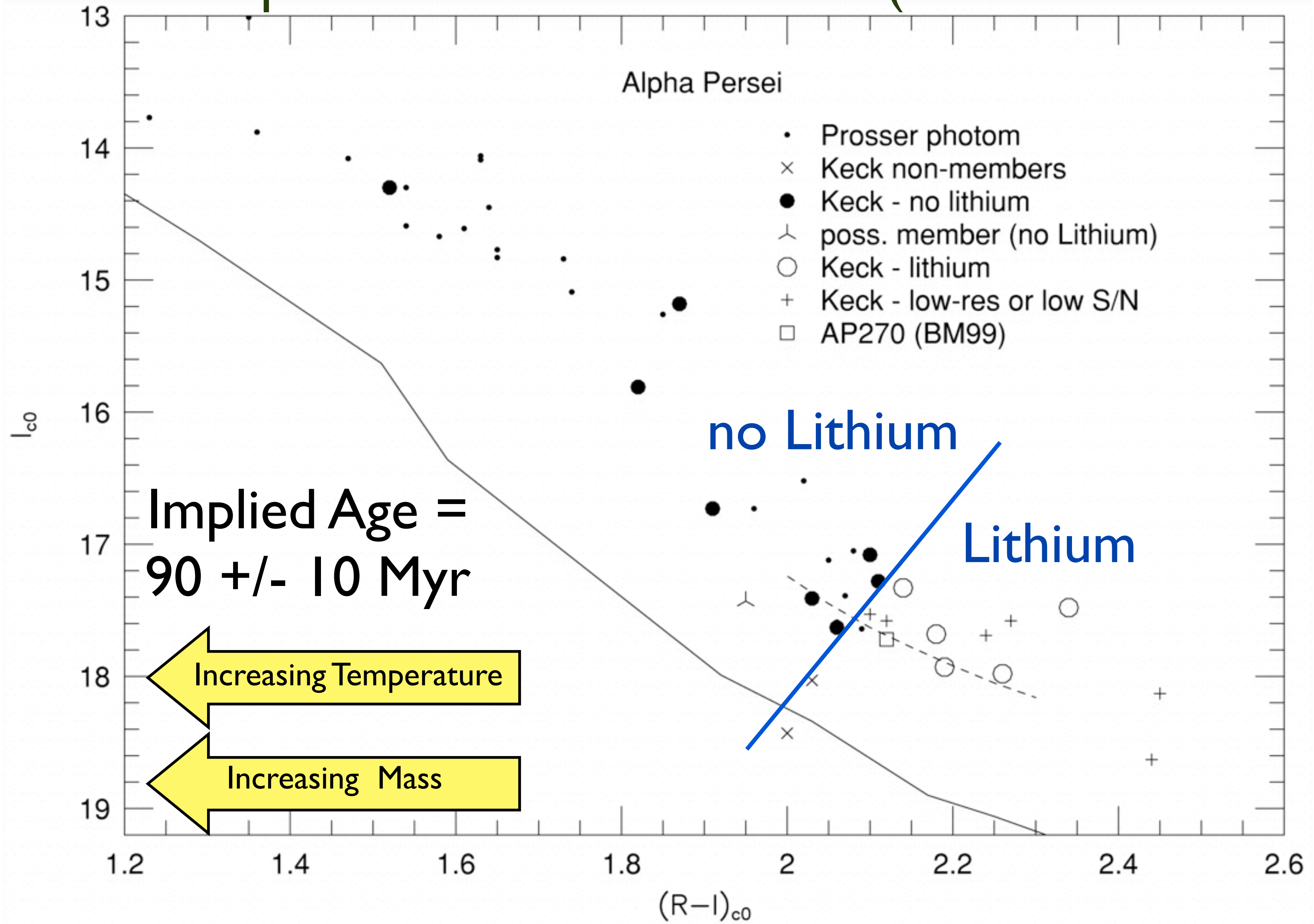

Summary

Previous to Silicon burning, only a limited number elements can be formed: H, C, O, Ne, Na, Mg, Al, Si, S

During the "silicon burning" phase, the temperatures and the energies of the gamma rays can photodisintegrate nuclei.

Elements grown through capture of α and other particles, growing elements to Nickel.

Star can enter nuclear statistical equilibrium, where elemental abundances are determined by a Saha equation for proton and neutron capture. For high enough temperature, Iron disintegrates back into Helium.

Production of neutrons can lead to s-process (neutron capture slower than beta decay). This produces primarily stable elements where the number of protons and neutrons are very similar. In supernova, high neutron densities can lead drive r-process. This can drive the production of more neutron rich isotopes and heavier elements.

Technetium is a short lived element that is found in the atmospheres of Mira variables. It is thought to form through the S-process and then transported to the atmosphere by convection.

In pre-main sequence stars, Lithium in low mass convective stars (without radiative zone) can be depleted by Lithium burning in core before the onset of Hydrogen burning.